

Electrochemical characteristics of HVOF spray coated layer with WC–27NiCr and WC–10Co4Cr for Al bronze

Min-su HAN, Seung-jun LEE, Min-sung KIM, Seok-ki JANG, Seong-jong KIM

Division of Marine Engineering, Mokpo Maritime University, Mokpo 530-729, Korea

Received 21 May 2012; accepted 16 October 2012

Abstract: Among the environmentally friendly marine energies, tidal current power plants require low cost because they do not need to construct a large dam. Tidal power is particularly reliable energy source because the power generation capacity is predictable regardless of weather or season. Composite materials or stainless steel have been used as materials of blades for current power plant. However, their strength and welding performance generated many problems in field application. Copper alloys with excellent cavitation resistance and corrosion resistance were applied as blade materials to improve the durability of copper alloys. They were coated with WC–27NiCr and WC–10Co4Cr using the high velocity oxy-fuel (HVOF) method. The metal spray coating technology has the advantage in terms of the selection of materials for cost effectiveness and environmental effects of corrosion because the properties of the coat layer can be controlled intentionally. Coating with WC–27NiCr and WC–10Co4Cr by HVOF, WC–27NiCr shows better corrosion resistance overall. The reason for this seems to be that corrosion resistance improves and a stable passive film forms due to the effects of Ni and Cr.

Key words: tidal power; copper alloys; HVOF coating; corrosion resistance

1 Introduction

Among the surface coating methods, the thermal spray technique sprays materials in molten or half-molten conditions at high velocity using a high temperature heat source. When this technique is used, the materials with excellent cavitation resistance and corrosion resistance can be replaced with low cost materials. It modifies the surface properties of coating materials with excellent characteristics, and the maintenance and repair of products are easy. At present, most materials that can be melted can be used as the thermal spray material. With the development of spray process technology, almost all materials are used including ceramics and carbide metals, etc. Among them, carbides such as WC and Cr_3C_2 which have high hardness are used in very wide applications due to their abrasion resistance, but they are a little brittle. When such elements as Co and Ni are added as metal binder, they show excellent abrasion resistance even at high temperatures from 500–800 °C. These materials are

widely applied to ships, airplanes, and power generation applications [1]. Furthermore, these materials are economical because they improve the durability by replacing highly brittle hard chrome plating [2,3]. The coating layer has been prepared by various spray coating processes such as gas flame spray, plasma spray, explosion spray, or high velocity oxy-fuel (HVOF) spray. Recently, HVOF spray method is mainly used which can form a compact coating layer due to relatively low thermal energy and the high kinetic energy of the flying particles [4]. The WC–Co alloys are composite materials that combine the WC strengthen phase with high hardness and strength and the metal Co binder with excellent toughness. It is widely implemented in machine processing, abrasion resistance and cutting tool parts in all industries [5–7]. To investigate the corrosion characteristics of the coating materials for copper alloys which can be applied to seawater environment WC–27NiCr and WC–10Co4Cr were coated on AC bronze using the HVOF method. Then, electrochemical experiments were conducted and the electrochemical characteristics were analyzed and compared through

Foundation item: Project supported by the Ministry of Education, Science Technology (MEST) and Korea Industrial Technology Foundation (KOTEF) through the Human Resource Training Project for Regional Innovation

Corresponding author: Seong-jong KIM; Tel: +82-10-57213722; E-mail: ksj@mmu.ac.kr

DOI: 10.1016/S1003-6326(12)61799-3

scanning electron microscope (SEM).

2 Experimental

In this study, ALBC3 alloy with excellent durability in seawater environment was used as the base metal. The coating materials were sprayed by HVOF using WC–27NiCr and WC–10Co4Cr. The chemical compositions of the base metal and coating materials are listed in Tables 1 and 2. To make identical roughness of the surface of base metal, it was polished with paper No. 600. The optimized conditions for HVOF method of each material are shown in Table 3. All the electrochemical experiments were performed in natural seawater solutions. The natural potential measurement experiment was conducted for 86400 s (24 h) and the potential was measured by elapsed time. An Ag/AgCl electrode was used as the reference electrode, and a Pt electrode was used at the scan rate of 2 mV/s in natural seawater solution. The anodic polarization experiment was conducted from open circuit potential and the cathodic polarization experiment was conducted from the open circuit potential to -2.5 V. The electrochemical experiment used multi-channels. The potentiodynamic experiment of ± 250 mV for the open circuit potential was applied; the corrosion potential and the corrosion current density were compared by Tafel analysis. The potentiostatic experiment was conducted for 3600 s at a constant potential to evaluate the microscopic corrosion characteristics with applied potential. The behavior of current density was analyzed during the experiment and the surface damages were observed with SEM.

Table 1 Chemical composition of ALBC3 alloy (mass fraction, %)

Al	Fe	Ni	Zn	Sn	Pb	Si	Mn	Cu
9.30	3.66	4.39	0.34	0.01	0.013	0.17	0.55	Bal.

Table 2 Chemical composition of HVOF coating materials WC–27NiCr and WC–10Co4Cr

Material	Mass fraction/%				
	Cr	Ni	Co	C	W
WC–27NiCr	20	7	–	5	68
WC–10Co4Cr	3.5–4.5	–	9–11	5.0–5.4	79.1–82.5

Table 3 Spray condition of atmospheric pressure plasma coating for WC–27NiCr and WC–10Co4Cr

Powder	Spray rate/ ($\text{g}\cdot\text{min}^{-1}$)	Spray distance/ mm	Feeder speed/ ($\text{r}\cdot\text{min}^{-1}$)	Gun barrel/ mm
WC–27NiCr	76	380	150	101.6
WC–10Co4Cr	100	380	200	203.2

3 Results and discussion

Figure 1 shows the measurements of natural potential for 86400 s in seawater for the base metal and the WC–27NiCr and WC–10Co4Cr coating layers. In the early stage of immersion, the base metal showed the potential of -0.21 V immediately after immersion and maintained stable values until the end of experiment. The WC–27NiCr coating showed a noble potential immediately after immersion and rapidly moved to the active direction. After 4800 s, it showed the active potential of -0.24 V and maintained stable values until the end of experiment. The WC–10Co4Cr coating quickly presented an active potential from the noble direction at the early stage of immersion. After 6700 s, it showed the active potential of -0.303 V and maintained stable values until the end of experiment. The stabilized natural potential values varied with the influences of Ni and Co. Ni is known to have excellent corrosion resistance and oxidation resistance [8], and Co is known to improve abrasion resistance and oxidation resistance [9,10]. This effect seems to be due to the characteristics of the alloy elements. It appears that WC–27NiCr showed a nobler potential than WC–10Co4Cr due to the Ni elements which have a nobler potential.

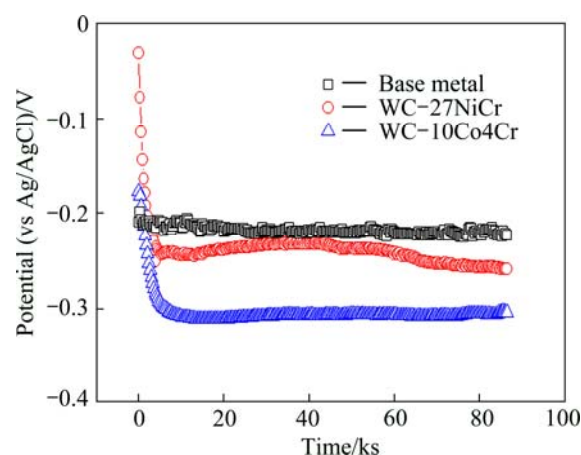


Fig. 1 Variation of potential for WC–27NiCr and WC–10Co4Cr during 86400 s in seawater

Figure 2 presents the anodic polarization tendency of the base metal, the WC–27NiCr and WC–10Co4Cr coating layers in seawater environment. The current density of the base metal increased from the open circuit potential (ϕ_{oc}) to $+0.1$ V. Then, it decreased to 1.3 V, which is a passivation characteristic. The WC–27NiCr coating layer clearly showed passivation characteristics from the open circuit potential (ϕ_{oc}). Then, the current density rapidly increased at 0.6 V as the coating layer was destroyed.

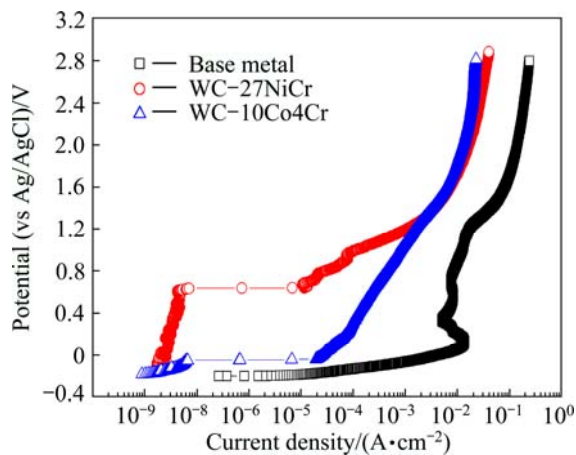


Fig. 2 Anodic polarization curves for WC-27NiCr and WC-10Co4Cr in seawater

At potentials after 0.6 V which is a pitting corrosion potential, the current density is increased by active dissolution reaction and it steadily increased along with the increasing potential. On the other hand, the current density of WC-10Co4Cr rapidly increased at -0.05 V. Then the current density steadily increased along with the rising potential. Consequently, for the ALBC3 base metal, the corrosion matters formed on the surface due to active dissolution reaction during the anodic polarization seem to be the factor causing such passivation characteristics. On the other hand, the WC-27NiCr coating layer showed passivation characteristics from open circuit potential with stable behaviors in seawater. The active dissolution reaction following the early rising potential of the two coating materials is believed to be a selective corrosion that mainly occurs in the Ni and Co elements. Furthermore, both the materials showed very low current density compared to the base metal. This is appropriate for improvement of corrosion resistance in the corrosion condition.

Figure 3 describes the cathodic polarization tendency of the base metal, WC-27NiCr and WC-10Co4Cr coating layers in seawater environment. The base metal showed the initial potential of -0.2 V followed by a concentration polarization due to the reduction reaction of dissolved oxygen ($O_2 + 2H_2O + 4e \rightarrow 4OH$) and an activation polarization section by the generation of hydrogen gas ($2H_2O + 2e \rightarrow H_2 + 2OH^-$) [11]. The concentration polarization by the reduction reaction of dissolved oxygen was observed in the range of about -0.4 V to -1.0 V. Thereafter, the current density increased by the influence of activation polarization. Furthermore, when the impressed current cathodic protection system was applied, the turning point of the concentration polarization and activation polarization which corresponded to limit potential was -1.0 V. The WC-27NiCr and WC-10Co4Cr spray coatings showed

lower current density than the base metal in the concentration polarization section by the reduction reaction of dissolved oxygen. Thus, both materials had better corrosion resistance than the base metal. To compare the turning points of the concentration polarization by the reduction reaction of dissolved oxygen and the activation polarization by the generation of hydrogen gas, it was -0.95 V for WC-27NiCr and -0.8 V for WC-10Co4Cr. Overall, the WC-27NiCr spray coating showed better characteristics than the WC-10Co4Cr spray coating.

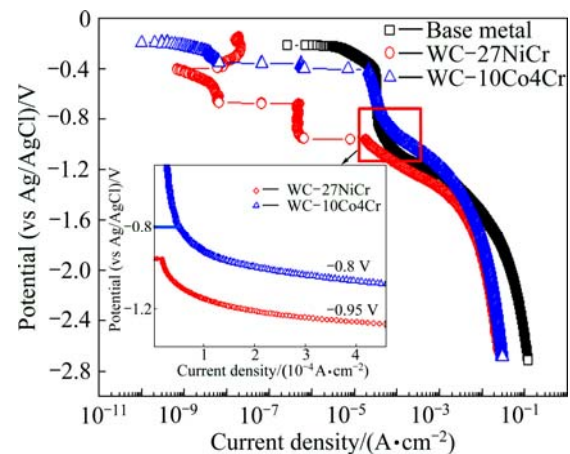


Fig. 3 Cathodic polarization curves for WC-27NiCr and WC-10Co4Cr in seawater

Figure 4 compares a ± 250 mV polarization graph at the open circuit potential for Tafel analysis. The current density gradually increased as the cathodic polarization curve moved in the active direction. An observation of the anodic polarization tendency found that the WC-10Co4Cr coating exhibited passivation characteristics after the open circuit potential, and its current density rapidly increased after pitting corrosion at around -0.08 V. Meanwhile, the WC-27NiCr coating showed passivation characteristics and a low current

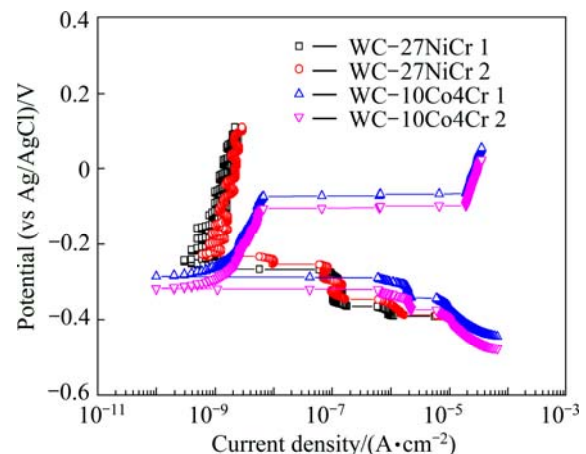


Fig. 4 Polarization curves for Tafel analysis of WC-27NiCr and WC-10Co4Cr in seawater

density from the open circuit potential. Table 4 lists the averages of corrosion potentials and corrosion current densities from the experiment.

Figure 5 shows the current density vs time curves for the WC–27NiCr coating layer after potentiostatic experiment at various potentials for 3600 s in seawater environment. In the range from 0.4 V to 1.2 V (Fig. 5(a)), generally high current densities were observed at 1.2 V as the anodic polarization curve, and the current density increased along with the increasing potential. At the potential of 0.6 V, the current density remained constant at $1.5 \times 10^{-5} \text{ A/cm}^2$ from the start to the end of immersion. At the applied potential of 0.4 V, however, the current

density was low, repeatedly rose and fell. In 0.4 V, the current density was the lowest at $6.7 \times 10^{-7} \text{ A/cm}^2$. In the range of applied potential from 0.2 V to 0.2 V (Fig. 5(b)), the current density dropped in the early stage of immersion in 0.2 V and showed stable behavior until the end of experiment. At 0V and 0.2 V, the current density dropped after immersion, and as the applied potential decreased, the current density gradually decreased while repeatedly rising and falling. At the range of applied potential from 0.8 V to 0.4 V (Fig. 5(c)), the current densities are repeatedly fluctuated from the start to the end of experiment. In the range of applied potential from 1.5 V to 1.0 V (Fig. 5(d)), the current density increased

Table 4 Tafel analysis result for WC–27NiCr and WC–10Co4Cr in seawater

Experiment No.	WC–27NiCr		WC–10Co4Cr	
	Corrosion potential/mV	Corrosion current density/($\text{A} \cdot \text{cm}^{-2}$)	Corrosion potential/mV	Corrosion current density/($\text{A} \cdot \text{cm}^{-2}$)
1	–307.7	8.425×10^{-8}	–302.7	6.066×10^{-7}
2	–233.9	3.271×10^{-9}	–308.4	3.461×10^{-7}
Average	–270.8	4.376×10^{-8}	–305.5	4.7634×10^{-7}

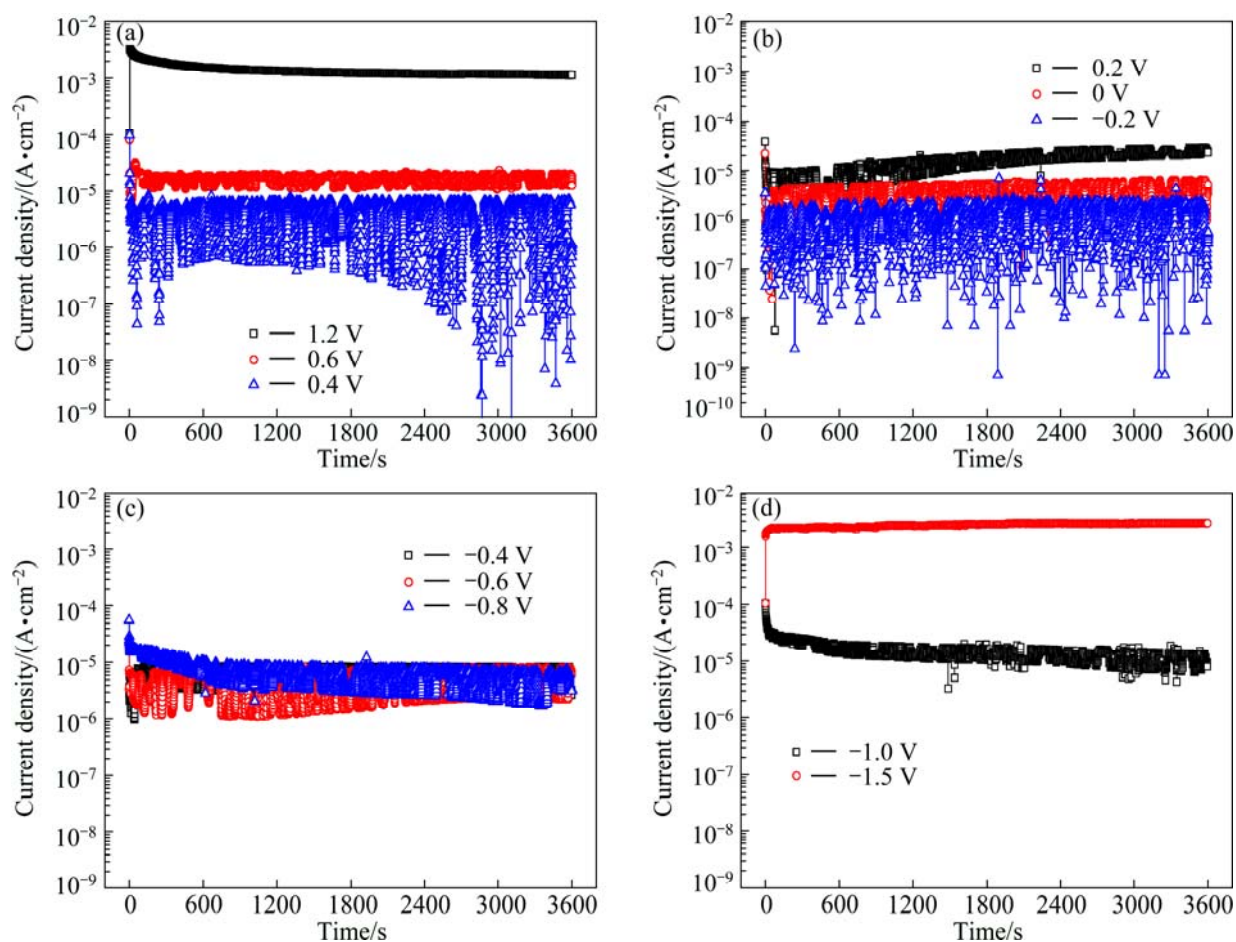


Fig. 5 Time—current density curves with various applied potential after potentiostatic experiments during 3600 s for WC–27NiCr coating in seawater: (a) 0.4 to 1.2 V; (b) –0.2 to 0.2 V; (c) –0.8 to –0.4 V; (d) –1.5 to –1.0 V

as the potential moved to the active direction, and the highest current density of $2.76 \times 10^{-3} \text{ A/cm}^2$ was observed at the lowest applied potential of 1.5 V. The reason that the current density increased as the potential decreased seems to be that the activation polarization tendency was more active as the potential decreased.

Figure 6 presents the current density with time of the WC-10Co4Cr coating layer after potentiostatic experiment at various potentials for 3600 s in seawater

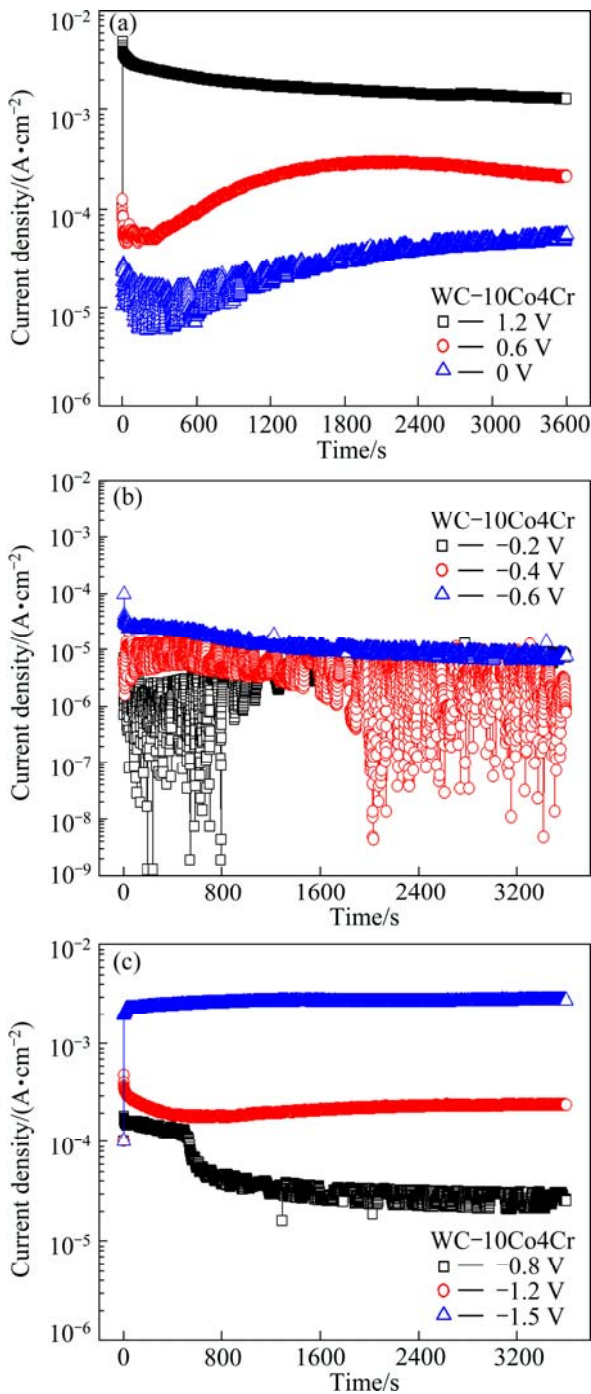


Fig. 6 Current density—time curves with various applied potentials after potentiostatic experiments during 3600 s for WC-10Co4Cr coating in seawater: (a) 0 to 1.2 V; (b) -0.6 to -0.2 V; (c) -1.5 to -0.8 V

environment. In the range from 0 V to 1.2 V (Fig. 6(a)), a high current density was observed at 1.2 V and the current density rapidly decreased in the early stage of immersion at 0.6 V, before gradually increasing after 250 s. At 0 V, the current density gradually increased while repeatedly rising and falling, and showed a relatively low value at $5.58 \times 10^{-5} \text{ A/cm}^2$ at the end of experiment. In the range (b) from -0.6 V to -0.2 V (Fig. 6(b)), the current densities are repeatedly fluctuated after immersion and showed a low value at -0.2 V and -0.4 V. At -0.6 V, the current density gradually decreased over time after immersion and became low. In the range of potential from -1.5 V to -0.8 V (Fig. 6(c)), the current stayed constant at -0.8 V and rapidly fell at 490 s before stabilizing at 600 s. Then the experiment ended at a relatively low current. At -1.2 V and -1.5 V, the current density tended to increase as the current moved in the active direction.

Figure 7 compares the current density between the WC-27NiCr and WC-10Co4Cr coating layers after the potentiostatic experiment for 3600 s in natural seawater solution. The WC-27NiCr coating layer showed the lowest current density at the applied potential of -0.2 V, whereas the WC-10Co4Cr coating layer showed the lowest current density at the applied potential of -0.4 V. These values are close to the natural potential of each coating. Almost symmetrical behavior appeared when they were anodically or cathodically polarized. WC-27NiCr showed better corrosion resistance as its current density was lower than that of WC-10Co4Cr at most applied potentials.

Figure 8 shows the surface morphologies for the WC-27NiCr and WC-10Co4Cr coating layers after the potentiostatic experiment for 3600 s in natural seawater solution. The potential generally increased, the

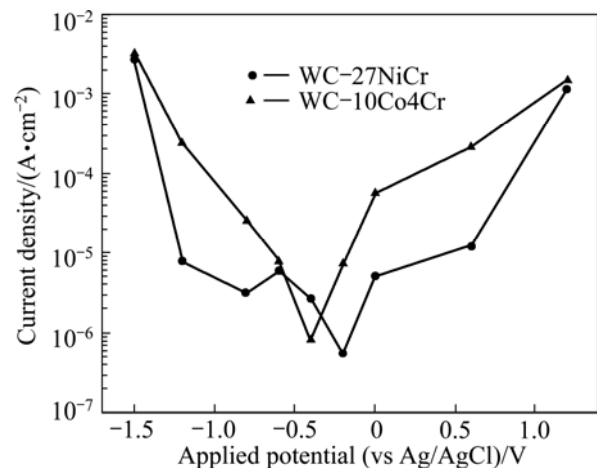


Fig. 7 Comparison of current densities after potentiostatic experiment for 3600 s in seawater

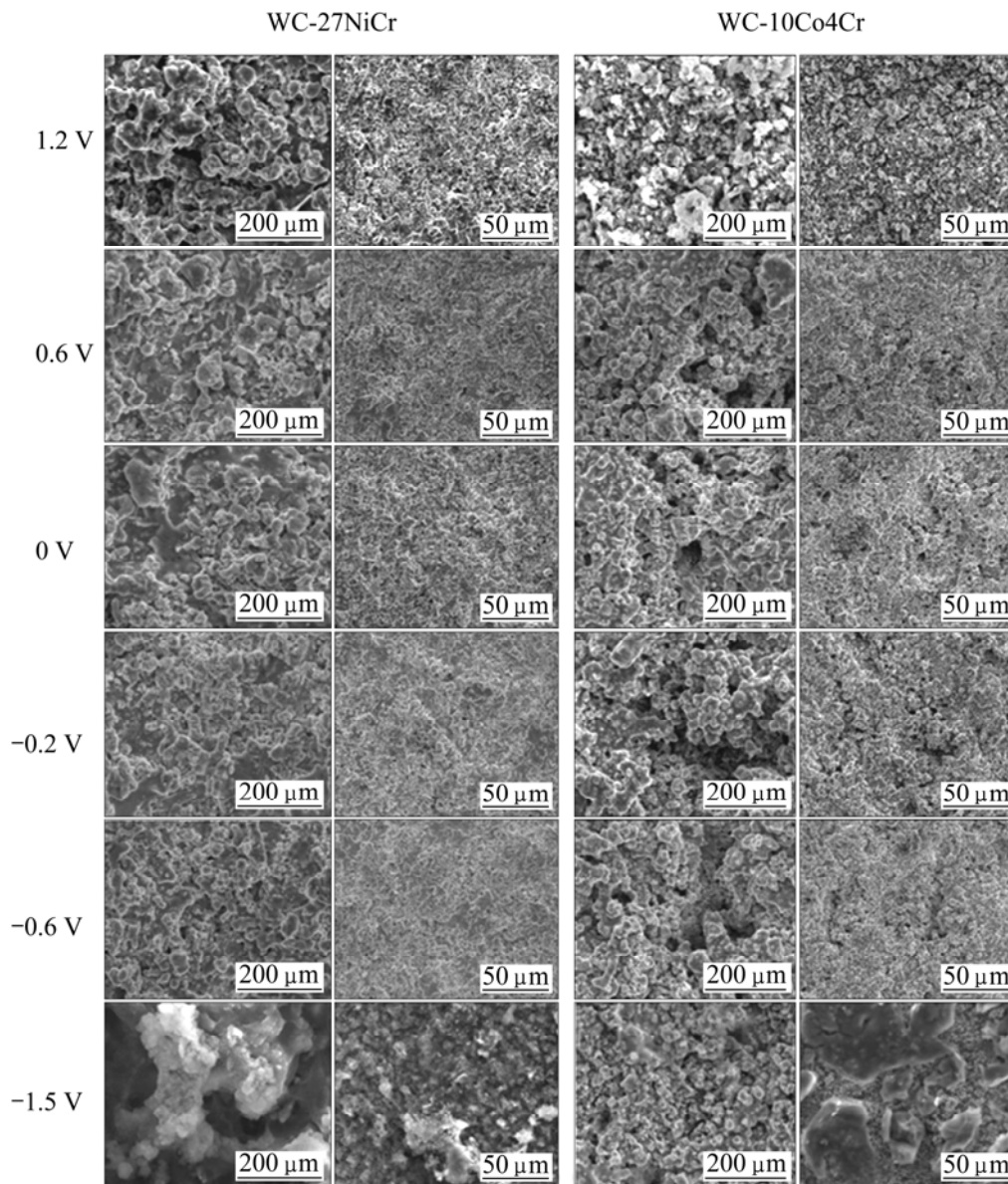


Fig. 8 Surface morphologies of WC-27NiCr and WC-10Co4Cr with various applied potential after potentiostatic experiments during 3600 s in seawater

dissolution reaction was activated and the corrosion damages increased. At 1.2 V, harsh corrosion was observed on the specimen surface by active dissolution reaction as discussed in the potentiostatic experiment. In the potential range of -0.6 V to 0.6 V, on the other hand, a low current density appeared as it was a by passivation and concentration polarization section due to the reduction reaction of dissolved oxygen. As a result, the surface was almost free of damages in general. In the case of WC-10Co4Cr, the coating layer was damaged due to characteristics of the activation polarization by active dissolution reaction and the generation of hydrogen gas at 1.2 V and -1.5 V. During the potentiostatic experiment at each applied potential, WC-27NiCr showed less damages. Synthetically, the

WC-27NiCr showed better electrochemical behaviors from all the test observations.

4 Conclusions

- 1) Both coating materials showed very stable natural potential behavior in the seawater environment.
- 2) At the anodic polarization experiment, the WC-27NiCr coating showed passivation characteristics and a low current density from the open circuit potential. Meanwhile, the WC-10Co4Cr coating showed passivation characteristics after open circuit potential and its current density rapidly increased after pitting at around -0.08 V.
- 3) At the potentiostatic experiment, WC-27NiCr

showed lower current density than WC–10Co4Cr at most applied potentials, suggesting that it would exhibit better corrosion resistance. At the Tafel analysis, WC–27NiCr would exhibit better corrosion resistance as the corrosion current densities of WC–27NiCr and WC–10Co4Cr were 4.3760×10^{-8} A/cm² and 4.7634×10^{-7} A/cm², respectively.

References

- [1] RHYS-JONES T N. Thermally sprayed coating systems for surface protection and clearance control. Applications in aero engines [J]. Surf Coat Technol, 1990, 43–44(1): 402.
- [2] HWANG S Y, SEONG B G, LEE D S, PARK C K. Degradation behavior of WC base coatings in molten zinc [C]//15th International Therm Spray Conf. 1998: 25–29.
- [3] SARTWELL B D, BRETZ P E. HVOF thermal spray coatings replace hard chrome [J]. Adv Mater Proc, 1999, 8: 25–28.
- [4] THROPE R, KOPECH H, GAGNE N. HVOF thermal spray technology [J]. Adv Mater Proc, 2000, 157(4): 27–29.
- [5] BJORDAL M, BARDAL E, ROGNE T, EGGEN T G. Erosion and corrosion properties of WC coatings and duplex stainless steel in sand-containing synthetic sea water [J]. Wear, 1995, 186–187: 508–514.
- [6] TOMA D, BRANDL W, MARGINEAN G. Wear and corrosion behaviour of thermally sprayed cermet coatings [J]. Surf Coat Technol, 2001, 138: 149–158.
- [7] de SOUZA V A, NEVILLE A. Corrosion and erosion damage mechanisms during erosion-corrosion of WC–Co–Cr cermet coatings [J]. Wear, 2008, 255: 146–156.
- [8] FANG W, CHO T Y, YOON J H, SONG K O, HUR S K, YONG S J, CHUN H G. Processing optimization, surface properties and wear behavior of HVOF spraying Wc–CrC–Ni coating [J]. Journal of Materials Processing Technology, 2009, 209(7): 3561–3567.
- [9] KARIMI C H, VERDON G, BARBEZAT. Microstructure and hydroabrasive wear behavior of high velocity oxy-fuel thermally sprayed WC–Co coatings [J]. Mater Sci Technol, 1996, 81: 81–89.
- [10] MURTHY J K N, VENKATARAMAN B. Abrasive wear behavior of WC–CoCr and Cr₃C₂–20(NiCr) deposited by HVOF and detonation spray processes [J]. Surf Coat Technol, 2006, 200: 2642–2652.
- [11] KIM S J, JANG S K, KIM J I. Electrochemical properties and corrosion protection of stainless steel for hot water tank [J]. The Korean Journal of Chemical Engineering, 2004, 21(3): 739–745.

(Edited by LONG Huai-zhong)